

Copper Electrodeposition From Non-Polluting Aqueous Ammonia Baths

Magdy A.M. Ibrahim

Electrodeposition of copper from aqueous ammonia solutions onto steel substrates has been studied. This investigation includes detailed studies on the influence of bath composition, as well as the operating conditions for producing good quality copper deposits. It was found that the optimum conditions for producing bright copper deposits are: $\text{CuSO}_4 \cdot 5\text{H}_2\text{O}$ 80 g/L, NH_3 100 g/L, $(\text{NH}_4)_2\text{SO}_4$ 50 g/L, KOH 15 g/L and 3.0×10^{-5} mol/L SDBS (as an anionic surfactant) at $i = 2.7 \text{ A/dm}^2$, pH 10.5, and at 25°C . Moreover, the study includes potentiostatic current-time and cyclic voltammetry measurements carried out on a rotating carbon disc electrode. The surface morphology of the as-deposited copper was investigated by using scanning electron microscopy (SEM).

Plating of steel parts with copper before nickel and chromium plating is of commercial importance. Another large scale use of copper plating is in the electronic industry where, because of its conductivity, it is used to produce the millions of square feet of printed circuit boards used each year.¹ In addition, copper is an important metal in contributing to improved corrosion resistance of plated zinc die cast parts.²

Electrodeposition of copper is normally performed using cyanide-based baths. These baths have the disadvantage of being strong pollutants, however, because the cyanide ion is among the products obtained. For this reason, alternative baths have been extensively studied.³⁻⁹ Attempts have been made to electrodeposit copper and other metals from an electrolytic bath containing ammonium salt.^{7,10,11} The ammonia bath seems to be a good non-polluting alternative for copper electrodeposition from cyanide baths. Moreover, the

presence of ammonia or an ammonium salt not only offers homogeneity and brightness,¹² but also decreases the anodic corrosion.¹³

The aim of this study is to develop baths from which copper metal can be electrodeposited from ammonia solutions with good characteristics; also having the advantage of being more environmentally friendly than traditional cyanide baths. In addition, the study aims to throw light on the mechanism of copper electrocrystallization from the copper amine complex baths.

Experimental Procedure

All the plating bath constituents were reagent grade, using doubly distilled water. The composition of the baths used for copper electrodeposition is given in Table 1. For electrodeposition, a steel cathode and a platinum sheet anode, each of dimensions (2.5 x 3.0 cm) were used. The plating cell used was a rectangular Perspex trough (10 x 3.0 cm and 2.5 cm in height) provided with vertical grooves on each of the side walls to fix the electrodes. Before each run, the steel cathode was mechanically polished with different grade emery papers (600, 800, 1000 and 1500), then washed with distilled water, rinsed with ethanol, and weighed. The cathodic current efficiencies (CCE) were determined with the help of a coulometer, ($\text{CCE} = \text{Wt}_{\text{exp}}/\text{Wt}_{\text{theo}}$) where Wt_{exp} is the weight of the deposit obtained experimentally, and Wt_{theo} is the weight of the deposit calculated theoretically according to Faraday's law. Most of the experiments were carried out at $25 \pm 2^\circ \text{C}$. The plating duration was 10 min. The loss of ammonia was kept to a minimum by making the measurements within 20 min. after the solutions were prepared.

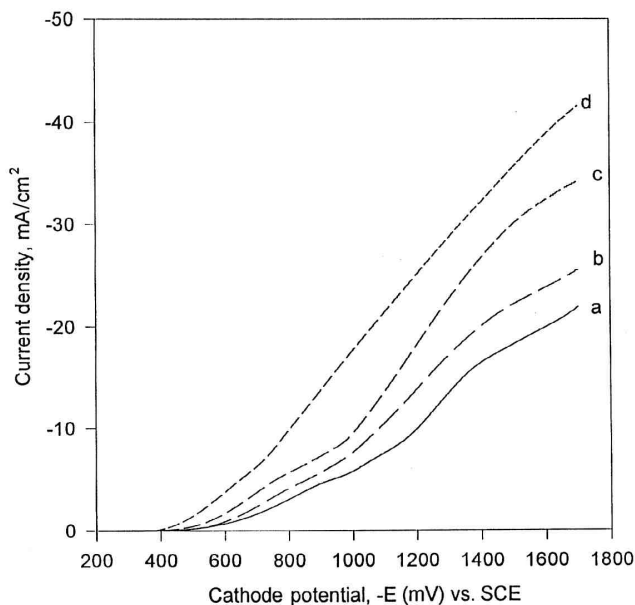


Fig. 1—Polarization curves during Cu electrodeposition from different solutions: curve a, bath No. 6; curve b, bath No. 5; curve c, bath No. 3; curve d, bath No. 4.

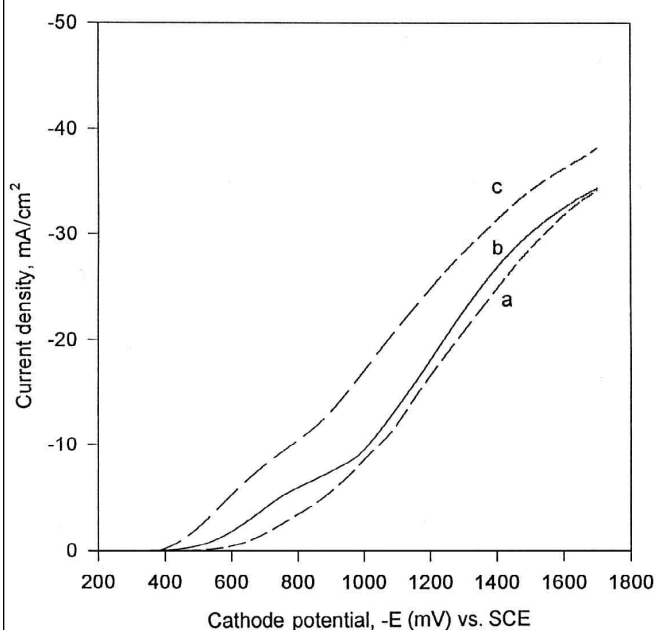


Fig. 2—Polarization curves during Cu electrodeposition from different ammonia solution concentrations: curve a, 190 g/L NH_3 ; curve b, 100 g/L; curve c, 80 g/L.

Potentiodynamic cathodic polarization measurements were performed in the rectangular cell. A potentiostat/galvanostat controlled by a PC was used for the potentiodynamic measurements. All potentials were measured relative to a saturated calomel electrode (SCE). To avoid contamination, the reference electrode was connected to the working steel cathode via a bridge provided with Luggin-Haber tip and filled with the solution under test. The tip was placed very close to the electrode surface.

The classic three-electrode cell was used for cyclic voltammetry measurements as well as for the current-potential curves measurements. The working electrode was a glassy carbon (area: 0.1963 cm²) rod embedded in a PVC cylinder. The carbon electrode was polished before each run with diamond paste (0.25 μm) until a mirror surface was obtained, then washed several times with doubly distilled water. The counter electrode was a small piece of platinum (area: 1.0 cm²). All the potentials were recorded with respect to a saturated calomel electrode placed in a Luggin capillary. Current transient measurements were performed in the usual manner with single potential steps.

The surface morphology of the copper electrodeposit was examined using scanning electron microscopy (SEM).

The microhardness of the copper deposit was measured by means of a microhardness tester. In this test, a 25 gf load was employed and the hardness was expressed as Vickers (H_v) in kg-force/mm².

Results & Discussion

Preliminary experiments were carried out to achieve suitable concentrations as well as suitable operating conditions for each of the bath constituents, as depicted in Table 1, to produce sound and satisfactory copper deposits. For example, electrodeposition of copper from a solution containing copper sulfate and ammonia solutions alone (Cu #1 bath), contains many bare areas (*i.e.*, the cathode surface is not completely covered by copper crystallites). Addition of ammonium sulfate (Cu #2 bath), however, to the previous solution greatly improves the compactness of the deposit.

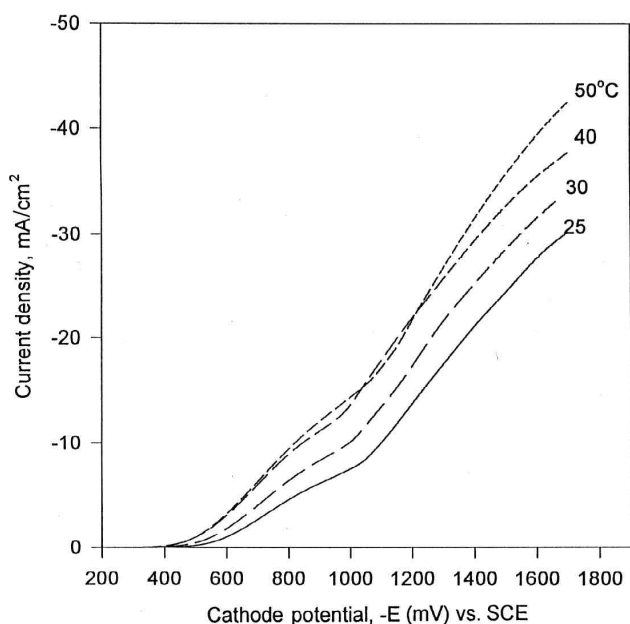


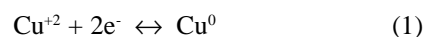
Fig. 3—Polarization curves during Cu electrodeposition from bath No. 8 at different temperatures.

On the other hand, decreasing ammonia concentration below 100 g/L (Cu #3 bath) results in the formation of a dull brick-red colored deposit at low current densities. This dull brick-red deposit phenomenon was previously obtained for the other baths but only at high current densities (> 4 A/dm²). Similar behavior is also well known for copper deposition from cyanide baths at high current densities.¹

KOH is normally added to increase the electrical conductivity of the bath.¹⁴ The quality of the deposit was rather improved by the addition of 3.0 x 10⁻⁵ M SDBS (sodium dodecyl benzene sulfonate) into the (Cu #8) bath. The deposit obtained from this bath was chosen as the optimum bath for producing sound and satisfactory copper deposits.

Potentiodynamic Cathodic Polarization Curves

In general, copper deposition from copper ions can be described by the following reaction:



Ammonium ions form soluble complexes with copper ions. The complex formed depends on the pH values. In the interval 7.7 < pH < 11.9, Cu⁺² ions predominate as Cu(NH₃)₄⁺².^{15,16} Copper complexation in the ammonia bath, therefore, is:



$$k_f = \frac{[\text{Cu}(\text{NH}_3)_4^{+2}]}{[\text{Cu}^{+2}][\text{NH}_3]^4} = 10^{15.7} \quad (3)$$

where k_f is the stability constant.¹⁷

Copper deposition from the ammonia bath can therefore be described as:

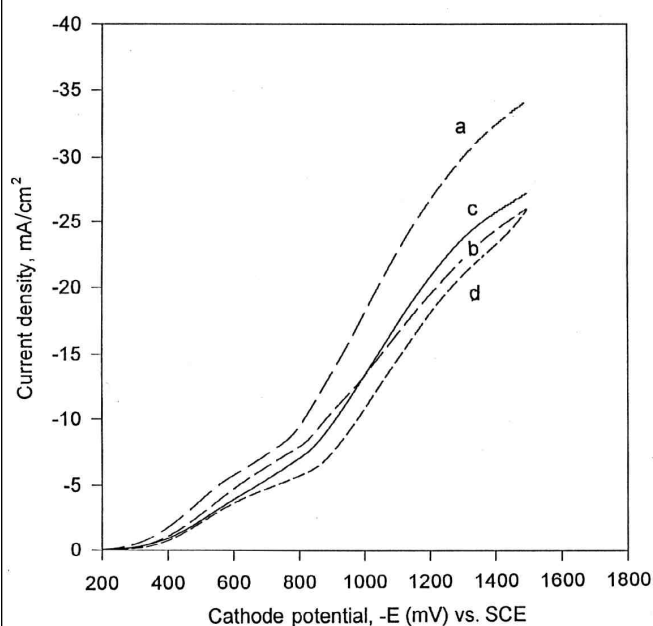


Fig. 4—Polarization curves during Cu electrodeposition with and without SDBS: curve a, 0.00; curve b, 1.5 x 10⁻⁵ M; curve c, 3.0 x 10⁻⁵ M; curve d, 7.5 x 10⁻⁵ M.

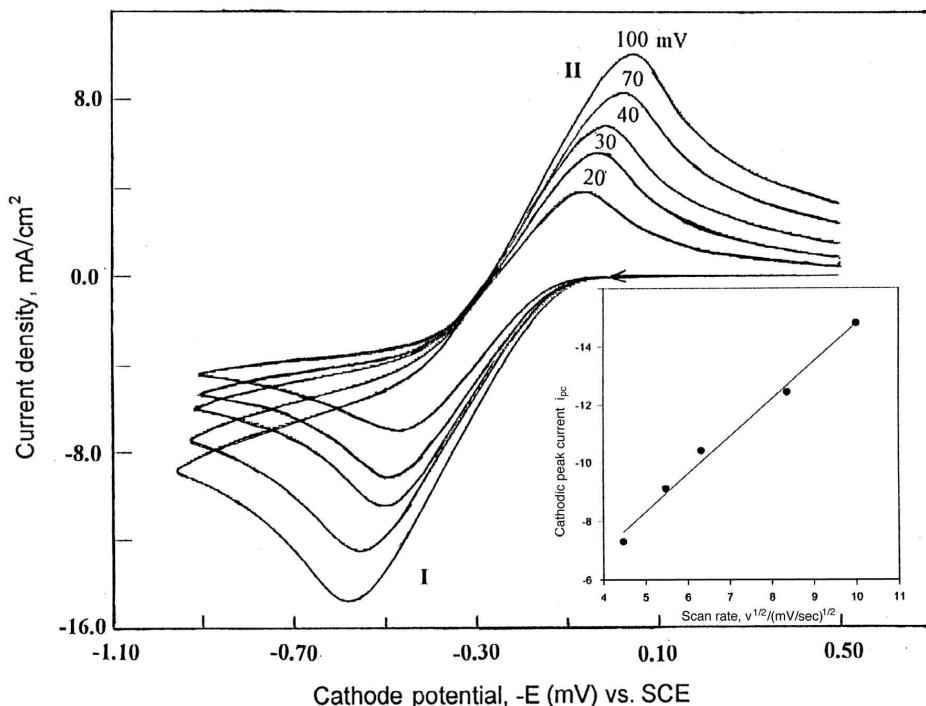
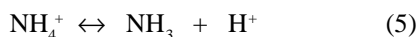


Fig. 5—Cyclic voltammety recorded at glassy carbon electrode for Cu #8 bath with different scan rate. Inset is the plot of cathodic peak current (i_{pc}) vs. square root of the scan rate ($v^{1/2}$).

Reduction of the copper amine complex is not as easy as the reduction of the free Cu^{2+} ions. This is the reason for the high polarization observed during Cu-electrodeposition from baths containing ammonia as shown in Figs-1-4. Moreover, the polarization curves show that the current tends to attain a limited value, especially at low Cu^{2+} ion concentration (Fig. 1), that results from the deposition limitation by the diffusion of Cu^{+2} ions.

On the other hand, the copper solution contains $(\text{NH}_4)_2\text{SO}_4$ in addition to NH_3 , because H^+ can be produced according to the following equation:



At sufficiently high negative potential values, therefore, further increase of the current density is observed as a result of the simultaneous hydrogen evolution. This reaction could produce a change in growth morphology of the deposit from an adherent deposit to a non-adherent, dull, brick-red deposit.¹⁸

Increasing the Cu^{+2} content in the bath, as shown in Fig. 1, greatly shifts the deposition potential toward the less negative values and enhances the limiting current values. These results could be attributed to the increase in the relative concentration of Cu^{+2} , particularly in the cathode diffusion layer, and this is reflected in a decrease in concentration polarization associated with copper deposition.

In contrast, increasing concentration of the ammonia solution shifts the cathodic polarization curves toward the more negative values (Fig. 2). This effect could be assigned to the decrease in the concentra-

tion of free Cu^{+2} as a result of complexation. On the other hand, addition of either KOH or ammonium sulfate has a very slight effect on the cathodic polarization curves (data are not included here).

The influence of temperature on the cathodic polarization curves during copper electrodeposition from Cu #8 bath was examined; the results are shown in Fig. 3. The data reveal that an increase in bath temperature shifts the polarization to the less negative values and enhances the limiting current values. This behavior could be related to the decrease in the activation overpotential of both hydrogen evolution and copper deposition reactions.¹⁹ Moreover, increasing temperature enhances the concentration of the reducible species in the diffusion layer as a result of increasing their diffusion rates.

Figure 4 shows the cathodic polarization curves for copper deposition, with and without addition

of different SDBS concentrations. It can be seen that the presence of SDBS results in a marked shift in the cathodic polarization toward more negative potential values and decreases the limiting current value. The inhibitory effect of SDBS could be a result of its adsorption on the metal surface, blocking the sites available for Cu deposition.

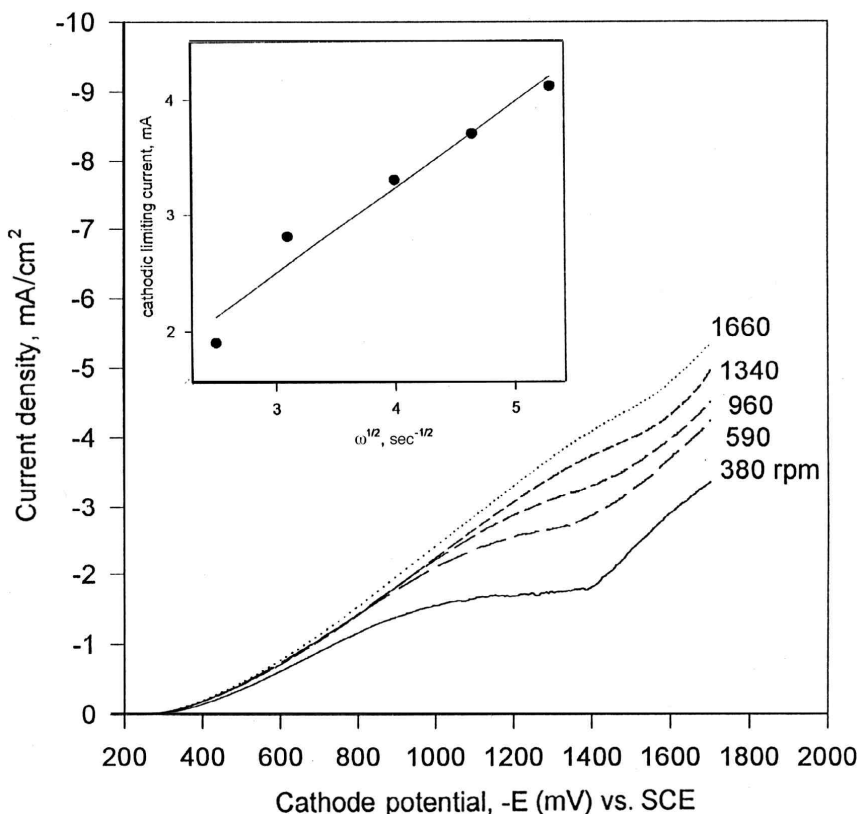


Fig. 6—Plots of current vs. potential at various rotation speeds for Cu #8 baths on glassy carbon disc electrode, scan rate 5 mV/sec. Inset is the plot of cathodic limiting current i_L vs. square root of the angular rotation $\omega^{1/2}$.

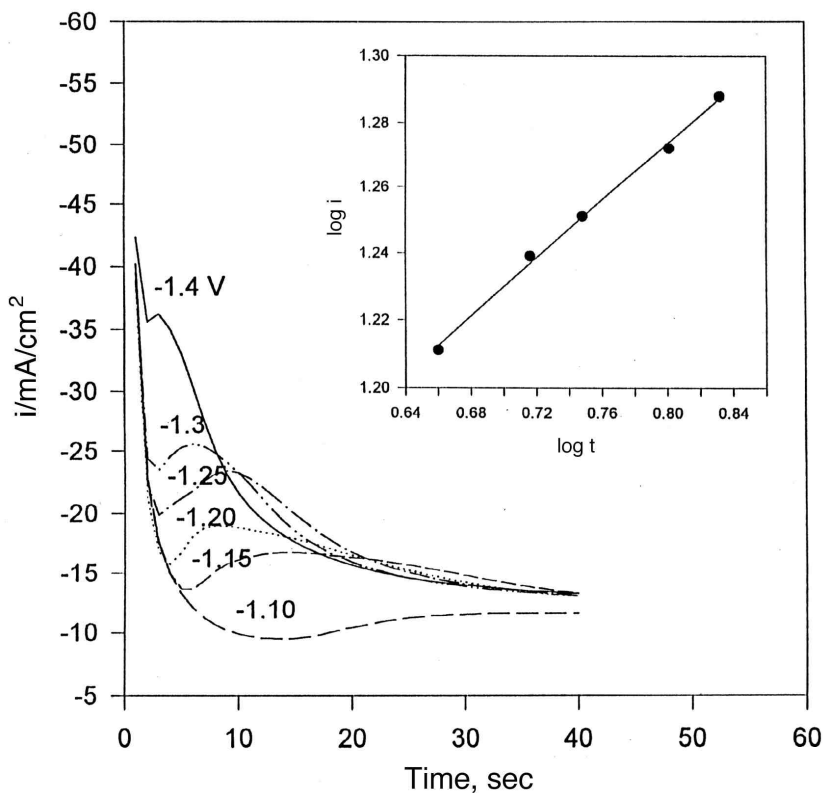


Fig. 7—Potentiostatic current-time transients from Cu #8 bath at various cathodic potentials. Inset is the plot of $\log i$ vs. $\log t$.

Cathodic Current Efficiency

The acid copper sulfate, copper fluoborate and copper pyrophosphate solutions have a CCE of 100 percent. On the other hand, cyanide-type copper plating solutions having CCE ranging from 50-90 percent depends upon the solution composition.¹ In our present baths, the behavior is similar to that of cyanide baths (*i.e.*, the CCE depends greatly upon the solution composition and the applied current density, as shown in Table 2). Inspection of the data in this table shows that addition of ammonium sulfate to Cu #1 bath increases the

Table 1
Composition of Copper Plating Solutions

Bath No.	CuSO ₄ ·5H ₂ O g/L	NH ₃ g/L	(NH ₄) ₂ SO ₄ g/L	KOH g/L	SDBS mol/L	C (Ω·cm) ⁻¹	pH
1	80	100	—	—	—	29.0	11.2
2	80	100	50	—	—	81.8	9.9
3	80	75	50	—	—	79.3	10.5
4	100	100	50	—	—	85.6	8.9
5	60	100	50	—	—	75.6	10.0
6	40	100	50	—	—	70.3	10.8
7	80	100	50	15	—	73.6	10.1
8	80	100	50	15	3 × 10 ⁻⁵	74.0	10.5

Table 2
Cathodic Current Efficiency Percent

Current A/dm ²	Bath No.							
	1	2	3	4	5	6	7	8
1.3	11.1	42.0	—	26.8	61.9	64.3	58.2	47.0
2.0	63.2	42.9	44.3	55.0	73.6	74.6	83.3	81.0
2.7	66.0	60.0	63.3	55.0	72.2	50.0	83.0	83.0
3.3	67.0	65.2	77.0	63.5	69.0	41.2	81.2	80.5
4.0	98.0	78.4	80.3	73	53.4	33.3	80.2	76.0

CCE only at low current density (1.33 A/dm²). With further increase in current density, CCE decreases gradually in comparison with those free from ammonium sulfate. Such a decrease has been observed as a result of (NH₄)₂SO₄ addition to a copper solution containing 1 M NH₄Cl.⁷ Moreover, inspection of the data in Table 2 indicates that increasing concentration of Cu⁺² content in the bath decreases CCE in all the current density ranges studied. These results contradict results found for copper deposition from other baths.^{20,21} This could be attributed to the fact that increasing Cu⁺² in a copper amine bath increases the stability of the complex formed (because of the presence of excess ammonia in the bath). As mentioned above, reduction from the complex species is not as easy as that for the free Cu⁺² ions. On the other hand, addition of KOH (Cu #7 bath) greatly improves the CCE.

In an attempt to improve the brightness of the copper deposit, SDBS was added (Cu #8 bath). The presence of SDBS in this bath had a slight decreasing effect on the CCE (see Table 2).

The effect of adding different concentrations of SDBS (3.0 × 10⁻⁵ to 4.5 × 10⁻⁴ M) on the CCE is given in Table 3, at $i = 2.7$ A/dm², pH 10.5, and 25 °C. It is obvious that only at

low concentrations range (3.0 × 10⁻⁵ to 4.5 × 10⁻⁵ M), the CCE is slightly increased with increasing SDBS concentration, then decreases to 79 percent, and finally levels off at about 76.7 percent.

Table 4 lists the effect of pH (range 9.5-12.5) on the CCE of copper electrodeposited from the Cu #8 bath. The pH was raised by using KOH solution. The data show that the CCE for copper deposits increases as the pH of the bath is increased from pH 9.5 to 10.5, and then levels off with further increase of pH.

Table 5 shows the effect of temperature on the CCE of copper electrodeposited from Cu #8 bath. Increasing temperature from 25 to 40 °C greatly decreases the CCE from 83.8 to 53 percent. It should be noted that at temperature ≥ 50 °C, no deposition of copper takes place from these baths.

From these results, it is found that the optimum

Table 3
Effect of SDBS on Cathodic Current Efficiency Cu #8 Bath

SDBS, mol/L	CCE, %
0.0	80.8
3.0 × 10 ⁻⁵	83.8
4.5 × 10 ⁻⁵	84.0
6.0 × 10 ⁻⁵	79.0
7.5 × 10 ⁻⁵	76.7
9.0 × 10 ⁻⁵	76.7
4.5 × 10 ⁻⁵	76.7

Table 4
Effect of pH on Cathodic Current Efficiency Cu #8 Bath

pH	CCE, %
9.5	72.9
10.5	83.0
11.5	82.3
12.5	84.3

Table 5
Effect of Temperature on Cathodic Current Efficiency Cu #8 Bath

Temp., °C	CCE, %
25	83.0
35	58.0
40	53.3

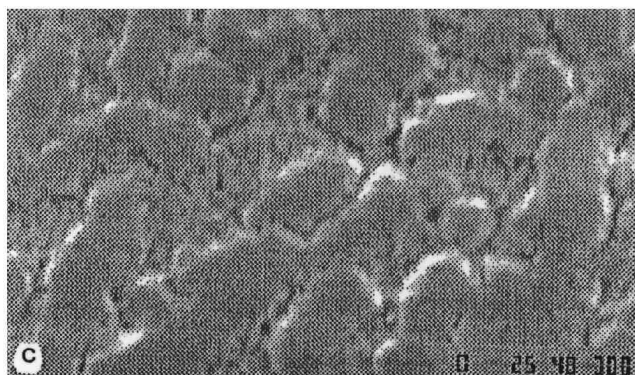
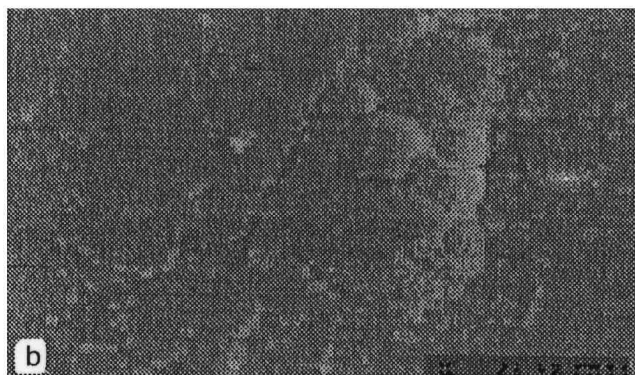
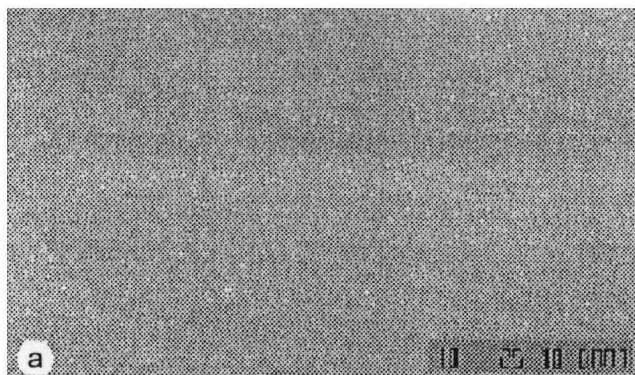


Fig. 8—Photomicrographs of deposited copper from various solutions:
 a. $\text{CuSO}_4 \cdot 5\text{H}_2\text{O}$ 80 g/L, NH_3 100 g/L, $(\text{NH}_4)_2\text{SO}_4$ 50 g/L, KOH 15 g/L, and 3.0×10^{-5} mol/L SDBS, at $i = 2.7 \text{ A/dm}^2$, pH 10.5, 25 °C. 2000X.
 b. $\text{CuSO}_4 \cdot 5\text{H}_2\text{O}$ 80 g/L, NH_3 100 g/L, $(\text{NH}_4)_2\text{SO}_4$ 50 g/L, KOH 15 g/L, at $i = 2.7 \text{ A/dm}^2$, pH 10.5, 25 °C. 2000X.
 c. $\text{CuSO}_4 \cdot 5\text{H}_2\text{O}$ 80 g/L, NH_3 100 g/L, $(\text{NH}_4)_2\text{SO}_4$ 50 g/L, KOH 15 g/L, and 3.0×10^{-5} mol/L SDBS at $i = 2.7 \text{ A/dm}^2$, pH 9.5, 25 °C. 2000X.

conditions for producing sound and satisfactory copper deposits are: $\text{CuSO}_4 \cdot 5\text{H}_2\text{O}$, 80 g/L, NH_3 solution, 100 g/L, $(\text{NH}_4)_2\text{SO}_4$, 50 g/L, KOH, 15 g/L and 3.0×10^{-5} mol/L SDBS (Cu #8 bath) at $i = 2.7 \text{ A/dm}^2$, pH 10.5 and 25 °C. Although the CCE of the present alkaline bath is not 100 percent, it is still higher (83.0 percent) than those reported for other copper alkaline baths, such as pyrophosphate³ and cyanide baths.²

Cyclic Voltammetry

A typical cyclic voltammogram of copper recorded at a glassy carbon electrode using the optimum Cu #8 bath under the influence of increasing scan rate (10-100 mV/sec), is shown in Fig. 5. The voltammetric studies were consistently performed in the potential range of 0.5 to 0.9 V. The sweep potential was initiated at 0.5 V and proceeded in the negative direction. The cyclic voltammogram exhibits two distinct voltammetric peaks (I and II). Peak (I) is associated with the Cu^{+2} reduction process (deposition), whereas peak (II) repre-

sents the dissolution of Cu deposited on the substrate.

The relationship between the cathodic current peak (i_{pc}) and the square root of the scan rate ($v^{1/2}$) (Fig.5) was found to be linear, indicating diffusion control; the rate of growth is controlled by mass transfer of copper ions to the growing center.⁶

Determination of the Diffusion Coefficient

To determine the diffusion coefficient for $\text{Cu}(\text{NH}_3)_4^{+2}$ species, the rotating disc electrode has been found to provide the most accurate method,^{22,23} using the Levich equation:

$$i_L = (0.62) nFAD^{2/3} \omega^{1/2} v^{-1/6} c \quad (6)$$

where ω is the angular rotation rate of the electrode (rad/sec), v is the kinematic viscosity ($9.85 \times 10^{-3} \text{ cm}^2/\text{sec}$) and c is the concentration of the electroactive species in the bulk of the solution. The dependence of the limiting current on the rotation speeds used in this study is shown in Fig. 6; the corresponding Levich plot with the limiting current i_L (measured at -1.2 V) is also shown in Fig. 6. The slope of the straight line obtained determines the value: $2.19 \times 10^{-7} \text{ cm}^2/\text{sec}$ for the diffusion coefficient. Most of the values recorded for the diffusion coefficient of Cu^{+2} in the literature are determined from aqueous acidic solutions.^{22,23}

Potentiostatic Current-Time Transients

A series of i - t transients for various values of the potentiostatic potential were performed for the Cu #8 bath on a glassy carbon electrode; the results are shown in Fig. 7. The decrease of the current in the first stage of the transient is related to the charge of the double layer.²⁴ The transients are characterized by the presence of a maximum current, i_{max} , which occurs at time t_{max} . T_{max} is related to the time at which full coalescence of the crystallites occurs.²⁵ The most interesting part of the i - t transients is the rising portion of the peak, which corresponds to the density before overlapping of the first monolayer of the growth nuclei and therefore can be used to determine the kinetics of nuclei growth.²⁶ The data show that as the potential is made more negative, i_{max} increases while t_{max} decreases. In principle, the dependence of i_{max} and t_{max} on the potential suggests that the rate of growth of nuclei is controlled by mass transfer. These results are in good agreement with those obtained by cyclic voltammetric technique (Fig. 5). By plotting $\log i$ vs $\log t$ for the rising part of the transient, therefore, the value of the measured slope is a constant depending primarily on the geometry and type of nucleation. An example of plotting $\log i$ against $\log t$ is also given in Fig. 7 (the curve corresponding to -1.20 V in Fig. 7). The straight line has a slope of 0.45, which is close to 0.5, indicating instantaneous nucleation.²⁷ This means that the formation of fresh nuclei is arrested at a very early stage. The same conclusion is also found during copper deposition from other, different baths.^{5,21,28}

Surface Morphology

Visual observation showed that the Cu deposits from the Cu #8 bath is bright, smooth, and red in color. The surface morphology of the as-deposited Cu was examined by scanning electron microscopy (SEM). Some of the SEM micrographs of the as-deposited copper under different operating conditions are shown in Fig. 8. The microscopic examinations of the as-deposited copper from the Cu #8 bath (Fig. 8a) at $i = 2.7 \text{ A/dm}^2$, pH 10.5 at 25 °C, composed of compact, non-porous and very fine grains covering the whole surface of the

cathode. Fig. 8b, however, shows that the absence of SDBS in the bath results in an increase in grain size. The great improvement in the uniformity and leveling in the Cu-deposit in the presence of SDBS (Fig. 8a) could be attributed to the increase in cathodic polarization (see Fig. 4). It is probable that the formation of fine grains is enhanced by any factor that increases the cathodic polarization.²⁹

On the other hand, it was observed that the surface morphology of the deposits varied from a fine grain structure (Fig. 8a) to a coarse grain structure as the pH of the bath was decreased from 10.5 to 9.5 (Fig. 8c).

Microhardness

Copper deposited from the optimum Cu #8 bath at $i = 2.7 \text{ A/dm}^2$ and pH 10.5 show a microhardness of 140 (kg/mm^2), while decreasing pH from 10.5 to 9.5 shows a decrease in the microhardness to 90 kg/mm^2 . This result is in good agreement with the result of the photomicrograph that shows relatively coarse-grained copper deposits at pH 9.5. This could be attributed to the fact that fine-grained deposits are harder than coarse-grained deposits.³⁰ Similar decrease of microhardness with lowering of pH was recorded for other metals.^{31,32} It is worthwhile to mention here that copper deposited from pyrophosphate shows hardness ranging from 83 to 250 (kg/mm^2), while copper deposited from acidic solutions show hardness ranging from 48-159 (kg/mm^2). This means that the hardness of the as-deposited copper at the optimum composition and at pH 10.5 is comparable to those of copper deposited from pyrophosphate, as well as from acidic solutions.

Summary

Fine-grained, highly adherent copper plates of red color can be deposited using the optimum bath: $\text{CuSO}_4 \cdot 5\text{H}_2\text{O}$, 80 g/L; NH_3 , 100 g/L; $(\text{NH}_4)_2\text{SO}_4$, 50 g/L; KOH, 15 g/L; and $3.0 \times 10^{-5} \text{ mol/L}$ SDBS at $i = 2.7 \text{ A/dm}^2$; pH 10.5 at 25 °C and duration 10 min. Under these conditions, the cathodic current efficiency was found to be strongly dependent on bath composition, as well as on the operating conditions such as pH, current density and temperature. The polarization curves show a remarkable polarization during copper deposition as a result of the formation of a stable Cu-amine complex. A value of $2.19 \times 10^{-7} \text{ cm}^2/\text{sec}$ was calculated for the diffusion coefficient of $\text{Cu}(\text{NH}_3)_4^{+2}$ by using a rotating disc electrode. Potentiostatic i-t, as well as cyclic voltammetry measurements confirmed that the deposition process takes place under diffusion control. The microhardness of the copper deposit under the optimum conditions has a value of 140 kg/mm^2 . The surface morphology of the as-deposited copper was investigated by SEM, with the results revealing that the copper deposits from the optimum conditions are composed of compact, non-porous, fine grains covering the whole surface of the cathode.

Editor's note: Manuscript received, October 1999. Revision received, January 2000.

References

1. F.J. Essex, *The Canning Handbook of Surface Finishing Technology*, E. & F.N. Spon Ltd., New York, 1985; pp. 522, 530, 525.
2. F.A. Lowenheim, *Modern Electroplating*, Wiley Interscience, New York, 1963; p. 165.
3. M. Ishikawa, H. Enomoto, M. Matsuoku & C. Iwakura, *Electrochim. Acta*, **40**(11), 1663 (1995).
4. Y. Fujiwara & H. Enomoto, *Surf. & Coat. Technol.*, **35**, 101

- (1988).
5. J. Crousier & I. Bimaghra, *Electrochim. Acta*, **34**(8), 1205 (1989).
6. T. Otero, *J. Appl. Electrochem.*, **29**(2), 239 (1999).
7. C. Nila & I. Gonzalez, *J. Electroanal. Chem.*, **401**(1-2), 71 (1996).
8. P. Fricoteaux, *Electrochim. Acta*, **44**(17), 2927 (1999).
9. A. Survila, *Soviet Electrochem.*, **28**(12), 1443 (1992).
10. A. Serruya, B.R. Scharifker, I. Gonzalez, M.T. Oropeza & M. Palomar-Pardave, *J. Appl. Electrochem.*, **26**, 451 (1996).
11. T.M. Tam & J.S. Zevely, *J. Electrochem. Soc.*, **131**, 109 (1984).
12. R. Winand, *Hydrometallurgy*, **29**, 567 (1992).
13. G.T. Burstein & R.C. Newman, *J. Electrochem. Soc.*, **128**, 2270 (1981).
14. J. Horner, *Plat. and Surf. Fin.*, **85**, 42 (Nov. 1998).
15. A. Rojas & I. Gonzalez, *Anal. Chim. Acta*, **187**, 279 (1986).
16. A. Rojas-Hernandez, M.T. Ramirez, J.G. Ibanez & I. Gonzalez, *J. Electrochem. Soc.*, **138**, 365 (1991).
17. L.G. Sillen & A.E. Martell, *Stability Constant of Metal-Ion Complexes*, The Chem. Soc., London, 1964; p. 152.
18. J.R. Roos, J.P. Celis & H. Kelchtermans, *Powder Technol.*, **20**, 139 (1978).
19. V.B. Singh & P.K. Tikoo, *Electrochim. Acta*, **22**, 1201 (1977).
20. F.H. Assaf, S.S. Abd El Rehim, A.S. Mohamed & A.M. Zaky, *Ind. J. Chem. Technol.*, **2**, 147 (1995).
21. Z.M.A. Ahmed, PhD Thesis, Suez Canal University (1997).
22. T.I. Quickenden & Qingzhong Xu, *J. Electrochem. Soc.*, **143**, 1248 (1996).
23. T.I. Quickenden & X. Jiang, *Electrochim. Acta*, **29**, 693 (1984).
24. G. Trejo, A.F. Gil & I. Gonzalez, *J. Appl. Electrochem.*, **26**, 1287 (1996).
25. J. Amblard, M. Froment, G. Maurin, D. Mercier, & E. Trevisen-Pikacz, *J. Electroanal. Chem.*, **134**, 345 (1982).
26. S. Fletcher, C.S. Halliday, D. Gates, M. Westcott, T. Lwin & G. Nelson, *J. Electroanal. Chem.*, **159**, 267 (1983).
27. C.Q. Cui, S.P. Jiang & A.C.C. Tseung, *J. Electrochem. Soc.*, **137**, 3418 (1990).
28. G. Fabricius, K. Kontturi & G. Sundholm, *Electrochim. Acta*, **39**, 2353 (1994).
29. S.S. Abd El Rehim, M.A.M. Ibrahim, S.M. Abd El Wahaab & M.M. Dankeria, *Trans IMF*, **77**(1), 31 (1999).
30. E. Raub & K. Muller, *Fundamentals of Metal Deposition*, Elsevier, Amsterdam, 1967; p. 203.
31. M.A.M. Ibrahim, S.S. Abd El Rehim, S.M. Abd El Wahaab & M.M. Dankeria, *Plat. and Surf. Fin.*, **86**, 69 (April 1999).
32. A.M. Abd El Halim, M.H. Fawzy & M.A.M. Ibrahim, *Trans. IMF*, **71**, 48 (1993).

About the Author



Dr. Magdy A.M. Ibrahim* is a lecturer of physical chemistry in the Chemistry Dept., Ain Shams University, Abbassia, Cairo, Egypt. He holds MSc and PhD degrees in electrochemistry from Ain Shams University. He held a scholarship in Germany at Erlangen-Nuremberg University (1992-1994). He is a UNESCO fellow for the 35th International Course for Advanced Chemistry and Chemical Engineering at the Tokyo Institute of Technology from October 1999 to September 30, 2000. He is an active member of the Egyptian Corrosion Society. His research interests include electroplating of metals and alloys, corrosion of metals and the electrochemistry of some organic compounds.

* Until September 30, 2000, Dr. Ibrahim may be contacted c/o Prof. Dr. Mashiro Yoshimura, Materials and Structure Laboratory, Tokyo Institute of Technology, 4259 Nagatsuda, Midori, Yokohama 226-8503, Japan